This research explores the use of SCARA robotic arms operated through Immersive Virtual Reality (IVR) interfaces, enhancing human-robot interaction for remote manipulation tasks. The problem addressed is the limited understanding of how non-expert users perform with such systems in teleoperation, compared to conventional control methods. While IVR offers immersive interaction, its effectiveness for users with limited teleoperation experience remains underexplored. To address this, an IVR-based system was developed to allow natural user interaction for executing pick-and-place tasks. Users control robotic arms in real time within a virtual environment using hand gestures and spatial interaction. Experimental evaluation involved twelve participants performing standardized tasks with both IVR and conventional interfaces. Performance was measured through execution time, success rate, and user experience using NASA-TLX and SUS metrics. The results show that the IVR reduces overall mental workload by approximately 45% and improves perceived usability by 15.9 points out of 100 compared to the traditional interface. Compared to conventional interfaces, participants completed tasks faster, with higher success rates and lower mental and physical demand. These improvements are due to the immersive nature of the IVR environment, which enhances spatial awareness and simplifies control of the robotic system. Real-time visual feedback further contributed to efficient interaction. The findings suggest the IVR interface is especially suitable for tasks requiring high operator involvement, such as remote manipulation in hazardous environments, training simulators, and educational robotics. Future work should optimize the interface for broader user tasks and capabilities

Keywords: immersive interface, robotic arm, mental workload, virtual reality, usability

UDC 004.896:004.94:681.518
DOI: 10.15587/1729-4061.2025.332483

EVALUATION OF AN IMMERSIVE VIRTUAL REALITY-BASED POSITION CONTROL INTERFACE FOR A SCARA ROBOTIC ARM

Victor Condori
Corresponding author
Bachelor Degree in Electronic Engineering*
E-mail: vcondoric@unsa.edu.pe
Jaime Castillo
Bachelor Degree in Electronic Engineering*
Alfredo Mamani
Bachelor Degree in Electronic Engineering*
Lizardo Pari
PhD Degree in Automation and Robotics*
*Department of Electronic Engineering
Universidad Nacional de San Agustin de Arequipa
Santa Catalina, 117, Arequipa, Peru, 04000

Received 29.05.2025
Received in revised form 16.07.2025
Accepted 04.08.2025
Published 29.08.2025

How to Cite: *Condori, V., Castillo, J., Mamani, A., Pari, L. (2025). Evaluation of an immersive virtual reality-based position control interface for a SCARA robotic arm. Eastern-European Journal of Enterprise Technologies, 4 (2 (136)), 110–116. https://doi.org/10.15587/1729-4061.2025.332483*

1. Introduction

The Selective Compliance Assembly Robot Arm (SCARA) continues to play a fundamental role in modern automation due to its speed, precision, and efficiency in tasks such as assembly, packaging, and material handling. Its applications have expanded into non-industrial domains as well, including agriculture, where it has been utilized for seeding, irrigation, fertilization, weeding, harvesting, and transportation [1]. As the demand for industrial automation grows, there is an increasing need for intuitive and efficient control interfaces that improve human-machine interaction, including the integration of immersive technologies such as Virtual Reality (VR) [2].

Immersive Virtual Reality (IVR) is characterized by high sensory fidelity and the ability to immerse the user in a psychologically convincing simulated environment, effectively isolating them from the physical world [3]. This form of interaction enables operators to control robotic platforms in real-time 3D spaces, offering a more natural and spatially aware alternative to conventional interfaces. Several initiatives have explored the creation of IVR-based systems to support natural human-robot interaction and facilitate the design and evaluation of such interfaces in generic usage contexts [4]. Additionally, IVR has proven effective in remote robotic operation scenarios under challenging conditions, such as limited bandwidth, where a single operator may manage semi-autonomous platforms [5].

Nevertheless, the IVR implementation in domains requiring high physical precision and mental focus – such as surgical training – has revealed certain limitations [6]. One recurring concern is the cognitive load imposed by immersive environments, which can lead to user skepticism, especially among operators accustomed to traditional methods. This distrust is exacerbated in high-stakes or physically demanding applications where IVR's impact on mental workload remains insufficiently studied [7]. Understanding these cognitive and ergonomic factors is essential to improving user confidence and advancing the adoption of IVR in robotic control systems. Therefore, research on immersive virtual reality-based control systems for robotic manipulators remains relevant.

2. Literature review and problem statement

Immersive virtual reality (IVR) has been increasingly applied to robotic control to improve spatial awareness and intuitive human-robot interaction. The paper [8] showed that IVR simulators can enhance robotics education by allowing students

to visualize and verify robot movements; however, their application remains limited to educational environments without real-time control over physical robots. In [9], a complete VR interface was connected to a robot controller, integrating mathematical models to enhance manipulation capabilities, but the evaluation of cognitive load and usability was not addressed.

To evaluate IVR systems, the paper [10] proposed a methodology based on physiological signals to assess user experience in autonomous systems, yet this approach focuses mainly on vehicle simulation contexts and may not generalize to robotic manipulation tasks. Similarly, [11] measured task performance and cognitive workload in pick-and-place operations using SUS and NASA-TLX. In [12], a vehicle-based simulator was used to improve immersion and reduce motion sickness compared to traditional VR; nevertheless, this research did not involve direct interaction with robotic manipulators.

The importance of multimodal feedback is highlighted in [13], where haptic systems were integrated into IVR to improve object manipulation, but such setups increase system complexity and cost, making them less viable for low-cost industrial applications. In [14], real-time robot control was implemented in an immersive environment to enhance user command intuitiveness in industrial settings; however, the study did not include standardized assessments of cognitive workload or usability.

All this allows to argue that it is appropriate to conduct a study devoted to evaluating an IVR-based interface for SCARA robotic arm control, focusing on usability, cognitive workload, and operational efficiency, with standardized evaluation methods under real teleoperation conditions.

3. The aim and objectives of the study

The aim of the study is to evaluate the feasibility and effectiveness of using an Immersive Virtual Reality (IVR) interface for position control of a SCARA robotic arm, with a focus on usability, accuracy, and mental workload during teleoperation tasks.

To achieve this aim, the following objectives were accomplished:

– to evaluate task performance through quantitative metrics such as execution time and success rate;

– to evaluate the cognitive workload experienced by users using the NASA Task Load Index (NASA-TLX) during teleoperation tasks;

– to assess the system's usability through the System Usability Scale (SUS) based on user feedback.

4. Materials and methods

4. 1. Object and hypothesis of the study

The object of this study is the immersive 3D interface on task execution time, error rate, mental workload, and perceived usability during pick-and-place tasks performed with a SCARA robotic arm.

The main hypothesis of the study is that the immersive 3D interface improves overall usability and reduces the operator's cognitive load, and also improves task performance compared to the conventional interface.

Assumptions made in the study include:

– participants share a comparable baseline level of familiarity with robotic interfaces;

– laboratory environment simulates real-world control conditions suitable for evaluating, it is assumed that the immersive system remains stable throughout testing and that environmental distractions are minimal;

– the control task is limited to position tracking along predefined pick-and-place trajectories, excluding dynamic or unstructured manipulation scenarios;

– the number of participants is restricted to a controlled sample group, which may not reflect the full diversity of potential end-users in real-world applications;

– only one robot type a 3D-printed SCARA arm is employed and a single immersive system configuration is used, without variation in hardware.

4. 2. SCARA robotic arm

Fig. 1 shows the kinematic model of a SCARA robot with three degrees of freedom. It includes the geometric and position variables required for its analysis listed in Table 1: heights (h_1), lengths (l_1, l_2), and joint angles (θ_1, θ_2). The reference frames (X_1, X_2) are defined according to the DH convention.

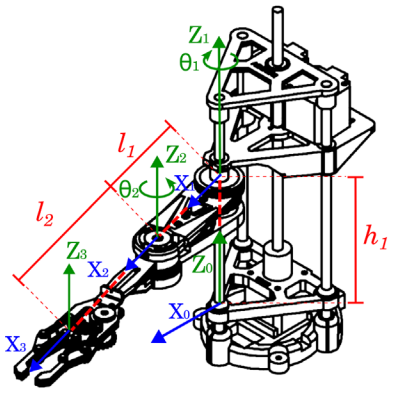

Fig. 1. Join axes and modeling of SCARA robotic arm

Table 1

SCARA robot parameters

Symbol	Description	Value
h_1	Height of the first link	0.5 m
l_1	Length of the first arm	1.0 m
l_2	Length of the second arm	0.8 m
θ_1	Rotation angle of the first arm	0° to 180°
θ_2	Rotation angle of the second arm	–90° to 90 °

Forward kinematics. The forward kinematics of the SCARA PRR robot is derived using the Denavit-Hartenberg (D-H) method used in [15, 16], which systematically represents the spatial relationship between consecutive links. This method uses four parameters for each joint: the joint angle θ_i, the link offset d_i, the link length l_i, and the twist angle α_i.

For the SCARA robot depicted in the reference figure, the D-H parameters are summarized in Table 2. The prismatic joint contributes a vertical displacement d_3, while the revolute joints define the planar motion through the angles θ_1 and θ_2.

Table 2

D-H Parameters for the SCARA PRR robot

Joint i	θ_i	d_i	$l_i(a_i)$	α_i
1	0	d_3	0	0
2	θ_1	0	l_1	0
3	θ_2	0	l_2	0

The homogeneous transformation matrix for each joint is derived based on the D-H parameters. These matrices describe the position and orientation of one link relative to the previous link. For the SCARA robot, the transformation matrices are as follows.

For the prismatic joint (Joint 1)

$$^0T_1 = \begin{bmatrix} 1 & 0 & 0 & 0 \\ 0 & 1 & 0 & 0 \\ 0 & 0 & 1 & d_3 \\ 0 & 0 & 0 & 1 \end{bmatrix}. \quad (1)$$

For the first revolute joint (Joint 2)

$$^1T_2 = \begin{bmatrix} \cos\theta_1 & -\sin\theta_1 & 0 & l_1\cos\theta_1 \\ \sin\theta_1 & \cos\theta_1 & 0 & l_1\sin\theta_1 \\ 0 & 0 & 2 & 0 \\ 0 & 0 & 0 & 1 \end{bmatrix}. \quad (2)$$

For the second revolute joint (Joint 3)

$$^2T_3 = \begin{bmatrix} \cos\theta_2 & -\sin\theta_2 & 0 & l_2\cos\theta_2 \\ \sin\theta_2 & \cos\theta_2 & 0 & l_2\sin\theta_2 \\ 0 & 0 & 1 & 0 \\ 0 & 0 & 0 & 1 \end{bmatrix}. \quad (3)$$

The total transformation matrix from the base {0} to the end-effector {3} is obtained by multiplying these individual matrices

$$^0T_3 = ^0T_1 \cdot ^1T_2 \cdot ^2T_3. \quad (4)$$

Expanding the product results in

$$^0T_3 = \begin{bmatrix} \cos(\theta_1+\theta_2) & -\sin(\theta_1+\theta_2) & 0 & l_1\cos\theta_1 + l_2\cos(\theta_1+\theta_2) \\ \sin(\theta_1+\theta_2) & \cos(\theta_1+\theta_2) & 0 & l_1\sin\theta_1 + l_2\sin(\theta_1+\theta_2) \\ 0 & 0 & 1 & d_3 \\ 0 & 0 & 0 & 1 \end{bmatrix}. \quad (5)$$

The position of the end-effector in Cartesian coordinates is extracted from the last column of the matrix:

$$x = l_1\cos\theta_1 + l_2\cos(\theta_1+\theta_2), \quad (6)$$

$$y = l_1\sin\theta_1 + l_2\sin(\theta_1+\theta_2), \quad (7)$$

$$z = d_3. \quad (8)$$

This derivation provides a complete representation of the forward kinematics, enabling the determination of the end-effector position given the joint variables θ_1, θ_2, and d_3. This formulation is essential for workspace analysis and motion planning of the SCARA robot.

Forward kinematics. The inverse kinematics of the SCARA PRR robot determines the joint variables θ_1, θ_2, and d_3 based on a given position of the end-effector in Cartesian coordinates (x, y, z). This process allows the robot to compute the joint motions required to reach a specific position, making it fundamental for tasks such as pick-and-place operations and trajectory planning.

The forward kinematics equations derived previously relate the joint variables to the end-effector position. Using these equations, the inverse kinematics problem is solved by isolating each joint variable. The vertical displacement d_3 is the simplest to determine, as it directly corresponds to the z-coordinate of the end-effector

$$d_3 = z. \quad (9)$$

To determine θ_2, it is possible to start by calculating the distance r from the base to the projection of the end-effector onto the XY-plane

$$r = \sqrt{x^2 + y^2}. \quad (10)$$

This distance (r) forms the hypotenuse of a triangle defined by the links l_1 and l_2. Using the law of cosines, θ_2 can be expressed as

$$r^2 = l_1^2 + l_2^2 - 2l_1l_2\cos\theta_2. \quad (11)$$

From this, the angle is calculated as

$$\theta_2 = \arccos\left(\frac{r^2 - l_1^2 - l_2^2}{2l_1l_2}\right). \quad (12)$$

With θ_2 determined, it is possible to proceed to calculate θ_1. Using the position equations in the XY-plane, θ_1 is given by

$$\theta_1 = a\tan 2(y,x) - a\tan 2(l_2\sin\theta_2, l_1 + l_2\cos\theta_2). \quad (13)$$

This expression accounts for the planar geometry of the SCARA robot and combines the contributions of both links to the position of the end-effector.

It is important to note that the robot may have two possible configurations for a given position, referred to as elbow-up and elbow-down configurations. These correspond to the positive and negative solutions for θ_2, respectively. The choice of configuration depends on the specific application or motion planning requirements.

Finally, to ensure the desired position is within the robot's workspace, the distance r must satisfy

$$r_{\min} \le r \le r_{\max}. \quad (14)$$

r falls outside this range, the position is not reachable, and the inverse kinematics problem has no solution.

The derived equations provide a complete and practical framework for solving the inverse kinematics of the SCARA PRR robot, enabling precise motion control and effective task execution within its workspace.

4. 3. Immersive interface integration

In this section, let's describe the integration of an experimental test platform designed to control a SCARA robotic arm. The process begins with the NUI interface, which allows users to set the desired position. This position is then projected into a virtual environment using Blender, where it is visualized and processed. Finally, the computed position is transmitted to the SCARA robot, enabling precise execution of the desired movement. Fig. 2 illustrates the overall pipeline of this integrated test interface.

The NUI and SCARA systems were developed with a combination of electronic and mechanical components to ensure accurate motion control. The NUI interface consists of sensors and microcontrollers that capture and process user inputs,

while the SCARA robot integrates actuators and structural elements to execute the commanded movements. Table 3 details the electronic components used and the proposed mechanical design for the test platform.

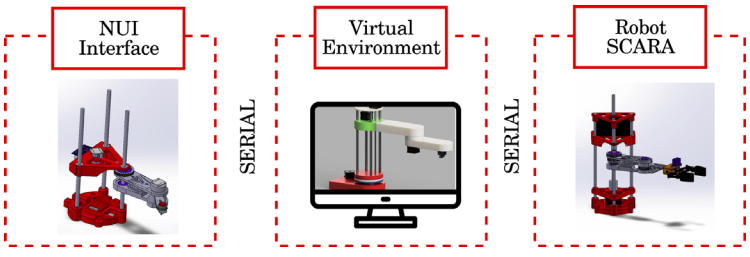

Fig. 2. Schematic diagram of the integrated test interface

Table 3

Component description of the NUI and SCARA systems

Component	Fig. Item	NUI	SCARA
Sensor	(1)	Encoders AS5600, Ultrasonic HC-SR04	–
Microcontroller	(2)	Arduino Mini Pro, Arduino Nano	Board GT2560, Arduino Mega
Actuator	(3)	–	Servo MG996R, Stepper motor 42SHD0034-20B
Peripheric	(4)	Push-button	–
Fixed base	(5)	Provides stability to the system and serves as support for three metal columns and the spindle motor	
Arms	(6.1), (6.2)	The total length of both extended arms is approximately 17 cm: – L1 (6.1): 9.5 cm, rotation from 0° to 180°; – L2 (6.2): 7.5 cm, movement from –90° to 90°	
Unfixed base	(7)	Moves along the Z-axis and supports electronic components	
Main axis	(8)	Three cylindrical supports with an 8 mm diameter	
Bearings	(9)	Allows free movement of the unfixed base	
Effector	(10)	Mounted at the end of arm L2, driven by a servomotor	

Fig. 3 illustrates the arrangement and organization of the components listed in Table III within the assembly of the NUI interface and the SCARA robot used in this study. This diagram details the structural layout and interconnections of each element, providing a comprehensive understanding of their functionality and potential for reuse.

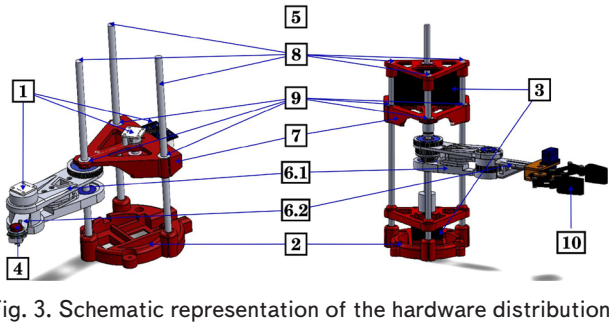

Fig. 3. Schematic representation of the hardware distribution in the NUI interface (left) and the SCARA robot (right). The numbers indicate: 1 — sensors; 2 — microcontrollers; 3 — actuators; 4 — push-button; 5 — fixed base; 6.1, 6.2 — arms; 7 — unfixed base; 8 — main axis; 9 — bearings; 10 — end-effector

This component distribution reveals a simple and low-cost hardware configuration, where the NUI interface mainly includes the sensory components, while the SCARA robot integrates the actuators and mechanical structure.

This distribution highlights the functional separation between perception and action modules, simplifying both the system's design and its implementation for teleoperated tasks.

5. Evaluation results of the IVR interface for SCARA robot teleoperation

5. 1. Quantitative result of task performance in IVR

The percentage of successfully completed tasks and the execution time were measured by the evaluators during task execution. The first evaluator provided instructions to the operators on the pick-and-place task, positioned the target object, and designated the final placement zone. Meanwhile, the second evaluator recorded execution times and documented successful and failed attempts. Each attempt in which the object was picked and placed in the designated area was considered a successful task. Conversely, a failed attempt was recorded if the object could not be picked up, was not placed near the target area, or if the operation exceeded ten minutes. Each task was repeated three times with each of the twelve participants.

The completion times of the twelve participants for both interface types are presented in Table 4. The times recorded in this table correspond to the three attempts performed by the operators.

Additionally, Table 5 presents a comparison of the number of mistakes made during the pick-and-place tasks using both interfaces.

Table 4

Task completion times for pick-and-place execution using a 3D interface and a conventional interface

Operator	3D interface			Conventional interface		
	Task 1 (s)	Task 2 (s)	Task 3 (s)	Task 1 (s)	Task 2 (s)	Task 3 (s)
1	420	445	468	470	490	512
2	430	452	477	485	496	521
3	442	435	460	490	501	525
4	425	440	475	475	489	514
5	435	432	465	485	499	528
6	428	460	478	479	492	510
7	422	448	457	482	502	512
8	445	439	452	485	502	510
9	439	458	480	488	498	502
10	429	433	468	479	489	499
11	438	445	472	476	493	527
12	421	441	459	473	481	514

Table 5

Comparison of mistakes made during pick-and-place tasks using a 3D interface and a conventional interface

Operator	3D Interface			Conventional Interface		
	Task 1 (s)	Task 2 (s)	Task 3 (s)	Task 1 (s)	Task 2 (s)	Task 3 (s)
1	1	0	1	2	1	3
2	2	2	2	1	2	2
3	0	1	1	2	1	1
4	1	0	1	0	0	2
5	1	2	0	1	2	3
6	0	1	3	1	1	3
7	1	0	2	2	2	3
8	0	0	1	2	1	3
9	2	2	1	1	2	2
10	0	1	2	1	0	3
11	1	2	2	0	1	3
12	1	0	2	2	1	3

To statistically evaluate these data, let's use the Shapiro-Wilk test to verify the normality of each dataset. The results indicate that the completion times for the conventional interface have a P-value of 0.277, while the P-value for the 3D interface is 0.149. Since both values are greater than the significance level of 0.05, the null hypothesis is not rejected, indicating that these data follow a normal distribution. Consequently, a parametric test could be used; however, for consistency, it is possible to apply the Wilcoxon test to determine if there were significant differences within each group of repeated measures and between both interfaces. For the conventional interface, the Wilcoxon test resulted in a P-value of 0.0005, indicating significant differences among repeated measures. Similarly, for the 3D interface, a P-value of 0.012 was obtained, confirming significant differences among repeated measures. Finally, when comparing both interface groups, the Wilcoxon test produced a P-value of 2.91×10^{-11}, which is significantly smaller than 0.05. This result indicates substantial differences in completion times between the two interfaces.

5. 2. Cognitive workload result

On the other hand, to assess interface performance in terms of cognitive load, the NASA-TLX questionnaire was employed. This questionnaire includes six subscales: mental demand, physical demand, temporal demand, performance, effort, and frustration. Additionally, the System Usability Scale (SUS) questionnaire was used, comprising ten questions on a Likert scale from one to five, where one represents "Strongly agree" and five represents "Strongly disagree". Each participant completed the questionnaires at the end of the pick-and-place tasks.

The results obtained from the NASA-TLX questionnaire are presented in Table 6, and the summary of the obtained averages is shown in Table 7. Each cell is represented using a color map based on a Visual Analog Scale (VAS), where 0 indicates a very low mental workload (green) and 100 represents a very high mental workload (red). In the table, the NASA-TLX questionnaire components are identified as follows:

– TXL-Q1: mental demand;
– TXL-Q2: physical demand;
– TXL-Q3: temporal demand;
– TXL-Q4: performance (higher score is better);
– TXL-Q5: effort;
– TXL-Q6: frustration.

The Shapiro-Wilk test indicated that the NASA-TLX scores followed a normal distribution, with $P = 0.089$ for the proposed interface and $P = 0.566$ for the conventional interface. Levene's test confirmed the homogeneity of variance between both groups $P = 0.586$. Since these conditions were met, an independent samples t-test was conducted, yielding a P value of 0.025. As this value is below the significance threshold of 0.05, it is concluded that there is a statistically significant difference in workload perception between the proposed and conventional interfaces.

Table 6

NASA-TLX questionnaire results for the 3D and conventional interfaces. Cell colors represent mental workload levels: 0 indicates a very low workload (green), and 100 represents a very high workload (red)

Op.	Cuesionario NASA TLX Interfaz 3D						Cuesionario NASA TLX Interfaz Convencional					
	TLX-Q1	TLX-Q2	TLX-Q3	TLX-Q4	TLX-Q5	TLX-Q6	TLX-Q1	TLX-Q2	TLX-Q3	TLX-Q4	TLX-Q5	TLX-Q6
1	50	40	30	70	35	25	80	70	60	55	75	65
2	55	35	25	75	40	30	85	65	55	50	80	70
3	40	30	35	80	30	20	70	60	65	45	70	55
4	45	45	40	65	50	35	75	75	70	60	85	75
5	50	50	30	85	35	25	80	80	60	50	75	65
6	35	40	20	90	30	20	65	70	50	40	70	55
7	45	35	25	80	40	30	75	65	55	45	80	70
8	50	30	35	75	35	25	80	60	65	50	75	65
9	55	45	40	70	50	35	85	75	70	55	85	75
10	35	50	30	85	30	20	65	80	60	40	70	55
11	40	30	35	90	35	25	70	60	65	50	75	65
12	50	40	25	80	40	30	80	70	55	45	80	70

Table 7

Average NASA-TLX scores

Interface	Q1	Q2	Q3	Q4	Q5	Q6
Proposed	45.83	39.17	30.83	78.75	37.5	26.67
Conventional	75.83	69.17	60.83	48.75	76.67	65.42

5. 3. System's usability result

Additionally, the results from the SUS (System Usability Scale) questionnaire are presented in Table 8. The data is visualized using a color-coded Likert scale, where 1 corresponds to total disagreement, 2 to disagreement, 3 to neutral, 4 to agreement, and 5 to total agreement. The SUS questionnaire consists of 10 items designed to assess the usability and user experience of the system:

– Q1: preference for frequent use of the system;

– Q2: perception of the system as unnecessarily complex;

– Q3: evaluation of the system as easy and straightforward to use;

– Q4: need for technical support to use the system;

– Q5: perception of the system as well-integrated and functioning correctly;

– Q6: identification of inconsistencies within the system;

– Q7: ease of learning to use the system;

– Q8: perceived effort required to use the system;

– Q9: confidence in using the system;

– Q10: perceived need for prior learning before effectively using the system.

The SUS score provides a reliable measure of perceived usability, incorporating both positive and negative statements to balance the assessment. A higher score indicates better usability and user satisfaction, while lower scores highlight potential areas for improvement.

The results of the Shapiro-Wilk test $P = 0.104$ for the proposed interface and $P = 0.473$ for the conventional interface) confirmed that the SUS questionnaire scores followed a normal distribution. Additionally, Levene's test indicated homogeneity of variance $P = 0.641$. Under these conditions, an independent samples t-test was performed, obtaining a P value of 0.031. Since this value is below 0.05, a statistically significant difference in usability scores between both interfaces is observed.

6. Analysis of cognitive load, usability, and task performance in immersive robotic teleoperation

The quantitative analysis presented in Tables 4, 5 demonstrates a clear performance improvement when using the 3D IVR interface compared to the conventional interface. Specifically, the statistically significant reduction in task completion time ($p = 2.91 \times 10^{-11}$) highlights the advantage of intuitive spatial control in virtual environments. This result can be explained by the fact that IVR allows operators to perform natural hand movements in three-dimensional space, reducing the cognitive load required to translate commands, as also observed in [10]. Additionally, the lower number of mistakes recorded with the 3D interface indicates better task execution accuracy, likely due to enhanced spatial awareness provided by the immersive system.

In terms of cognitive workload, Tables 6, 7 and the results of the NASA-TLX questionnaire show that the IVR interface reduces perceived workload compared to the conventional method ($p = 0.025$). This finding addresses the concern raised in Section 2 (Literature Review and Problem Statement) regarding user skepticism towards IVR systems due to unknown cognitive load effects, as previously noted by [7, 8]. Unlike traditional interfaces where users often experience high mental and physical demand, our results suggest that the immersive environment distributes cognitive effort more evenly across sensory and motor channels.

Regarding usability, Table 8 and the results of the SUS questionnaire reveal a statistically significant improvement in user satisfaction and system usability when using the IVR interface ($p = 0.031$). This contrasts with the findings of [13], where VR interfaces often suffered from usability issues due to complex interaction schemes, especially in manipulation tasks. Unlike in [9], where virtual interfaces were primarily focused on educational visualization without real-time control feedback, our analysis shows that the system provides a fully functional teleoperation experience with measurable benefits in both performance and user acceptance.

However, this study presents certain limitations:

1. The experimental setup was conducted in a controlled laboratory environment, which does not fully replicate the complexities of real industrial scenarios.

Table 8

SUS questionnaire responses for the conventional and 3D interfaces. Cell colors represent response levels: 1 corresponds to total disagreement (red), and 5 corresponds to total agreement (green)

Op.	Cuestionario SUS Interfaz Convencional										Cuestionario SUS Interfaz 3D									
	Q1	Q2	Q3	Q4	Q5	Q6	Q7	Q8	Q9	Q10	Q1	Q2	Q3	Q4	Q5	Q6	Q7	Q8	Q9	Q10
1	3	4	3	5	4	3	2	3	2	3	4	1	3	2	5	2	4	2	5	2
2	4	4	4	3	3	4	3	2	2	4	5	2	5	3	4	1	3	1	4	1
3	3	2	4	4	3	4	3	2	3	3	4	2	3	3	5	1	4	1	3	2
4	2	4	3	3	2	4	2	3	2	2	3	1	4	2	4	3	5	1	4	3
5	3	2	3	4	2	3	4	4	2	3	4	1	5	3	5	1	5	1	5	1
6	2	3	3	3	2	4	3	3	4	2	5	2	4	2	5	1	5	1	4	2
7	4	4	3	2	2	2	3	3	3	4	4	3	4	2	5	2	4	1	4	1
8	3	4	4	4	4	3	4	2	2	3	4	1	5	1	3	2	5	3	3	2
9	2	3	3	3	3	4	3	4	4	2	2	1	4	3	4	1	4	2	5	1
10	4	4	4	2	4	4	2	4	3	3	3	2	5	1	4	1	5	2	5	2
11	2	4	3	4	5	4	3	2	4	3	5	1	4	1	5	2	5	1	3	1
12	3	3	2	4	3	2	3	4	3	4	4	2	4	2	4	1	5	1	4	1

2. The low-cost hardware used, while beneficial for research accessibility, may also introduce performance limitations not present in professional-grade systems.

Future research should explore testing the system in real industrial environments, incorporating larger and more diverse user groups, and integrating additional feedback modalities, such as haptic cues, to further enhance operator performance and acceptance.

7. Conclusion

1. The study demonstrated that implementing and evaluating an immersive virtual reality interface for SCARA robotic arm control led to a 10.8% reduction in average total task execution time with the 3D interface. These results are attributed to the intuitive spatial mapping, lower control complexity, and enhanced environmental awareness provided by the immersive system.

2. A reduction of approximately 45% in cognitive load was observed when using the IVR interface, as indicated by the NASA-TLX results ($p = 0.025$). This contrasts with previous VR-based solutions, often limited by high cognitive demands.

3. System usability increased by 15.9 points out of 100, as shown by the SUS scores ($p = 0.031$). Unlike previous systems with low usability, the proposed interface achieved measurable gains in user acceptance among non-expert operators.

Conflict of interest

The authors declare that they have no conflict of interest in relation to this study, whether financial, personal, authorship or otherwise, that could affect the study and its results presented in this paper.

Financing

The study was performed without financial support.

Data availability

The data that support the findings of this study will be made available from the corresponding author upon reasonable request.

Acknowledgments

The authors would like to express their sincere gratitude to the Universidad Nacional de San Agustin de Arequipa (UNSA), Arequipa, Peru, for the institutional support provided throughout the development of this research.

References

1. Roshanianfard, A., Mengmeng, D., Nematzadeh, S. (2021). A 4-DOF SCARA Robotic Arm for Various Farm Applications: Designing, Kinematic Modelling, and Parameterization. Acta Technologica Agriculturae, 24 (2), 61–66. https://doi.org/10.2478/ata-2021-0010
2. Martín-Barrio, A., Roldán, J. J., Terrile, S., del Cerro, J., Barrientos, A. (2019). Application of immersive technologies and natural language to hyper-redundant robot teleoperation. Virtual Reality, 24 (3), 541–555. https://doi.org/10.1007/s10055-019-00414-9
3. J Bailey, J. O., Bailenson, J. N. (2017). Immersive Virtual Reality and the Developing Child. Cognitive Development in Digital Contexts, 181–200. https://doi.org/10.1016/b978-0-12-809481-5.00009-2
4. Bazzano, F., Gentilini, F., Lamberti, F., Sanna, A., Paravati, G., Gatteschi, V., Gaspardone, M. (2016). Immersive Virtual Reality-Based Simulation to Support the Design of Natural Human-Robot Interfaces for Service Robotic Applications. Augmented Reality, Virtual Reality, and Computer Graphics, 33–51. https://doi.org/10.1007/978-3-319-40621-3_3
5. Planthaber, S., Mallwitz, M., Kirchner, E. A. (2018). Immersive Robot Control in Virtual Reality to Command Robots in Space Missions. Journal of Software Engineering and Applications, 11 (07), 341–347. https://doi.org/10.4236/jsea.2018.117021
6. Eley, C. L., Palaniappan, V., Carter, A., Sogaolu, O., Horwood, J., Davies, M. et al. (2024). Randomized controlled trial of the CMR immersive virtual reality (IVR) headset training compared to e-learning for operating room configuration of the CMR versius robot. Journal of Robotic Surgery, 18 (1). https://doi.org/10.1007/s11701-024-01885-y
7. Sun, N., Botev, J. (2021). Intelligent autonomous agents and trust in virtual reality. Computers in Human Behavior Reports, 4, 100146. https://doi.org/10.1016/j.chbr.2021.100146
8. Román-Ibáñez, V., Pujol-López, F., Mora-Mora, H., Pertegal-Felices, M., Jimeno-Morenilla, A. (2018). A Low-Cost Immersive Virtual Reality System for Teaching Robotic Manipulators Programming. Sustainability, 10 (4), 1102. https://doi.org/10.3390/su10041102
9. Pérez, L., Diez, E., Usamentiaga, R., García, D. F. (2019). Industrial robot control and operator training using virtual reality interfaces. Computers in Industry, 109, 114–120. https://doi.org/10.1016/j.compind.2019.05.001
10. Morra, L., Lamberti, F., Prattico, F. G., Rosa, S. L., Montuschi, P. (2019). Building Trust in Autonomous Vehicles: Role of Virtual Reality Driving Simulators in HMI Design. IEEE Transactions on Vehicular Technology, 68 (10), 9438–9450. https://doi.org/10.1109/tvt.2019.2933601
11. Aguilar, W., Pari, L., Silva, Y., Espinoza, E. S., Ccari, L. F. C., Peña, R., Medina, N. O. (2024). Implementation of a Robotic Arm Control for EOD Applications Using an Immersive Multimodal Interface. IEEE Access, 12, 133632–133647. https://doi.org/10.1109/access.2024.3432401
12. Lee, H., Byun, W., Lee, H., Kang, Y., Choi, J. (2023). Integration and Evaluation of an Immersive Virtual Platform. IEEE Access, 11, 1335–1347. https://doi.org/10.1109/access.2022.3232949
13. Wonsick, M., Padir, T. (2020). A Systematic Review of Virtual Reality Interfaces for Controlling and Interacting with Robots. Applied Sciences, 10 (24), 9051. https://doi.org/10.3390/app10249051
14. Belei, O., Shtaier, L., Stasiuk, R., Mirzojeva, A. (2023). Design of the human-machine interface for the cleaning-in-place system in the dairy industry. Eastern-European Journal of Enterprise Technologies, 3 (2 (123)), 44–51. https://doi.org/10.15587/1729-4061.2023.282695
15. Ibrahim, B. S. K. K., Zargoun, A. M. A. (2014). Modelling and Control of SCARA Manipulator. Procedia Computer Science, 42, 106–113. https://doi.org/10.1016/j.procs.2014.11.040
16. Soyaslan, M., Uk, M. E., Ali Shah, F. B. S., Eldogan, O. (2018). Modeling, control, and simulation of a SCARA PRR-type robot manipulator. Scientia Iranica, 27 (1), 330–340. https://doi.org/10.24200/sci.2018.51214.2065